Open Archive Toulouse Archive Ouverte (OATAO)

OATAO is an open access repository that collects the work of Toulouse researchers and makes it freely available over the web where possible.

This is an author-deposited version published in: http://oatao.univ-toulouse.fr/
Eprints ID: 6492

To link to this article: DOI:10.1179/026708404225010748
http://dx.doi.org/10.1179/026708404225010748

To cite this version:

Alexis, Joël and Adrian, Denise and Masri, Talal and Petit, Jacques-Alain *Adherence of electrodeposited Zn-Ni coatings on EN AW2024 T3 aluminium alloy.* (2004) Surface Engineering, vol. 20 (n° 2). pp. 121-127. ISSN 0267-0844

Any correspondence concerning this service should be sent to the repository administrator: staff-oatao@listes-diff.inp-toulouse.fr

ADHERENCE OF ELECTRODEPOSITED Zn–Ni COATINGS ON EN AW2024 T3 ALUMINIUM ALLOY

J. Alexis, D. Adrian, T. Masri and J. A. Petit

The use of hexavalent chromium in surface treatments will be reduced in the future, as it is suspected to be carcinogenic. Electrodeposition of Zn–Ni, which is currently used on steel, represents a non-chromate alternative surface treatment for the corrosion protection of aluminium alloys. Zn–Ni coatings were electrodeposited onto an EN AW2024 T3 aluminium alloy sheet in a laboratory flow cell. To obtain several percentages of Ni in the coatings, solutions with different Ni^{2+} concentrations were used. The influence of a specific pretreatment to promote adherence, such as zincate immersion (109 g L^{-1} ZnO, 525 g L^{-1} NaOH) or phosphoric anodisation (36 wt-%H_3PO_4, 20°C) prior to electrodeposition was also investigated. The smoothness of the coating, measured on a three-dimensional roughness tester, increased when the percentage of Ni increased. This can be explained by a microstructural refinement observed using SEM and AFM. These microstructural changes are due to the evolution of the crystal structure of the coatings and can be observed by X-ray diffraction. The mechanical properties of the coatings (hardness and Young's modulus) were measured by microindentation and nanoindentation. The adherence of the coatings was tested by a scratch test and a three point bending test dedicated to coatings. The scratch behaviour of the coatings was a function of the percentage of Ni. The scratches observed indicate a ductile fracture for coatings with a low percentage of Ni and a brittle fracture for a high percentage of Ni. Bending tests demonstrated the favourable effect of pretreatments such as zincate immersion or phosphoric anodisation as well as adhesion enhancement as a function of increasing percentage of Ni. SE/503

The authors are in the Laboratoire Génie de Production, Ecole Nationale d'Ingénieurs de Tarbes, 47 avenue d'Azereix, BP 1629, 65016 Tarbes Cédex, France (e-mail: alexis@enit.fr). *Manuscript received 8 July 2003; accepted 14 January 2004.*

Keywords: *Aluminium alloy, Electrodeposition, Zinc–nickel coatings, Adherence*

INTRODUCTION

Currently, to protect aluminium alloys from corrosion and to promote paint adhesion, European aeronautical manufacturers apply a chromate treatment. However, this treatment uses hexavalent chromate, which is toxic. Zn–Ni coating, much used for corrosion protection of automobile steel sheets, represents a possible substitute treatment for the corrosion protection of aluminium alloys. Bories[1] showed that the best corrosion protection for aluminium is obtained with Zn–Ni coatings containing between 12 and 16%Ni. In the first part of this paper, new investigations are presented on the correlation between the chemical composition, structure and microstructure of Zn–Ni deposits on EN AW2024 T3 aluminium alloy, obtained in a cell set up to represent an industrial surface finishing tank, i.e. with static vertical electrodes. The second part is dedicated to the measurement of the coatings' mechanical properties by microindentation and nanoindentation and to the understanding of the adherence of electrodeposited Zn–Ni. The influence of the percentage of Ni in the coatings and of pretreatments such as zincate immersion or phosphoric anodisation are studied in detail. The mechanical tests used are a scratch test and a three point bending test specific to the assessment of coating adherence.

EXPERIMENTAL ASPECTS

Elaboration of coatings

Zn–Ni coatings were electrodeposited onto an EN AW2024 T3 aluminium alloy sheet in a laboratory flow cell. To obtain several percentages of Ni (from 4 to 16 wt-%) in the coatings, different Ni^{2+} ion concentrations were used (Table 1). The different steps of the usual pretreatment were: acetone cleaning and rinsing in distilled water, NaOH cleaning and rinsing in distilled water, HF/HNO_3 cleaning, rinsing in distilled water and air drying. The influence of specific pretreatments such as zincate immersion (100 g L^{-1} ZnO, 525 g L^{-1} NaOH) or phosphoric anodisation (36 wt-%H_3P0_4, 20°C) prior to electrodeposition to promote adherence were investigated.

Characterisation of deposits

The roughness of the samples was studied using a three-dimensional roughness tester. The area scanned represents 1 mm^2 with a 1 μm sampling rate on each axis. The evolution of the two roughness criteria R_a and *Sdr* was investigated. For studies of morphology and composition, SEM with EDX was used. The thickness was measured by SEM observations in cross-section. The crystal structure was established by

Table 1 Typical flow cell plating conditions, pH = 2, $T = 60$°C, current density 50A dm^{-2}, wt-%Ni on coating

	Bath composition, g L^{-1}		
Type of coating	$NiCl_2$	$ZnCl_2$	KCl
Zn–4%Ni	13	334	340
Zn–8%Ni	39	334	340
Zn–16%Ni	142·5	334	340

X-ray diffraction using standard $\theta-2\theta$ geometry and Cu K_α ($\lambda=0{\cdot}154054$ nm) radiation. Residual stresses were also determined by X-ray diffraction using the $\sin^2\psi$ method. The variation in lattice spacing for the family (552) of the γ phase was measured to calculate the residual stress. The wetting properties of the cleaned or pretreated substrate were studied by contact angle measurements using the Fowkes[2] procedure and the two liquid method.[3] This second method was used to avoid the pressure of the spreading out influence π_e. The contact angles between the water droplets and the solid surface were measured in a neutral environment of pure liquid octane.

The depth profiles were measured by SIMS (IMS-4f, CESAM laboratory) with simultaneous Ar^+ ion sputtering. To compare the mechanical behaviour of the coating as a function of the percentage of Ni and the pretreatment, four mechanical tests were performed: a microindentation test, a nanoindentation test, a scratch test and a three point bending test. The hardness of the multimaterial deposit/substrate was obtained under several loads between 25 and 300 g. It is known that, for coatings and for a large range of indentation loads, the apparent hardness H_c is the result of contributions from both substrate and coating. The absolute hardness of the deposit was calculated using analytical models (*see* Appendix) then checked in experiments by nanoindentation. The present work discusses the validity of the Buckle,[4] Jonsson–Hogmark[5] and the Chicot–Lesage models.[6] Buckle proposed a model based on a discrete description of the deformation under the imprint. The model of Jonsson–Hogmark is based on the load supporting areas of the imprint in the film and in the substrate. More recently, Chicot and Lesage sought to describe the plastic deformation under the indent in the film and in the substrate.

Young's modulus of the coatings was measured by nanoindentation tests to avoid the influence of the substrate. Several small indentations were made using a Berkovitch indenter, and the load P and the displacement were continuously recorded during a complete cycle of loading and unloading.[7] The stiffness of the upper portion of the unloading data is equal to

$$S=\frac{dP}{dh}=\frac{2}{\sqrt{\pi}}E_r\sqrt{A}$$

where A is the projected area of the elastic contact, and E_r is the reduced modulus equal to

$$\frac{1}{E_r}=\frac{(1-\nu^2)}{E}+\frac{(1-\nu_i^2)}{E_i}$$

where E and ν are Young's modulus and Poisson's ratio, respectively, for the specimen and E_i and ν_i the same parameters for the indenter.

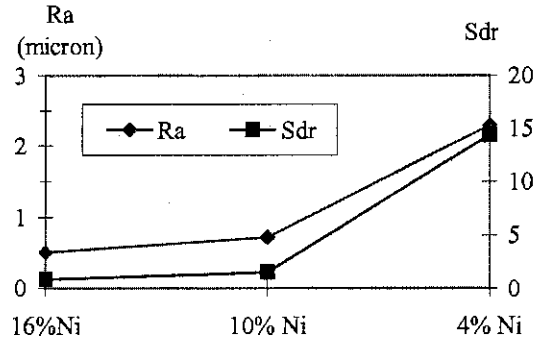

1 *Evolution of average arithmetic deviation R_a and of ratio of unfolded area Sdr versus type of coating*

The scratch test was performed using a microhardness tester instrumented with a translation table. A Vickers stylus was drawn across the sample at different loads between 15 and 500 g. Several testing parameters were fixed in order not to influence the results.[8] The scratch speed was 10 μm s^{-1}; the same indenter was used in order not to alter the indenter/surface interaction; all the samples were cleaned with alcohol before testing. The critical load was the load necessary to strip the coatings. The three point flexion test was performed on a tensile test apparatus with a specific assembly.[9] The sample dimensions and the test conditions were defined by the NFT 30010 standard. The stiffener, which was cured at ambient temperature, was a solvent free epoxy adhesive, CIBA AW 134/HM997. The average of the ultimate load F and its standard deviations were determined for eight samples for each different surface treatment.

RESULTS AND DISCUSSION

Topography and morphology

Roughness tests were performed for all the samples. As shown in Fig. 1, the average arithmetic deviation R_a and the ratio of unfolded area *Sdr* increases when the percentage of Ni in the coatings decreases. This behaviour is obviously the result of the coating morphology. Indeed, microstructural refining could be observed (Fig. 2) when the percentage of Ni increased. Several authors have observed similar results, which emphasise the influence of the percentage of Ni.[10,11] The Zn–8%Ni coating is microcracked (Fig. 2*b*). The microcracks go through the coating down to the substrate/coating interface. These microstructural changes can be explained by the evolution of the crystal structure of the coatings (Fig. 3). The diffraction analyses of the different coatings show that the microstructure of Zn–4%Ni is monophased η, the Zn–8–10%Ni coating are biphased η, γ and the coating containing

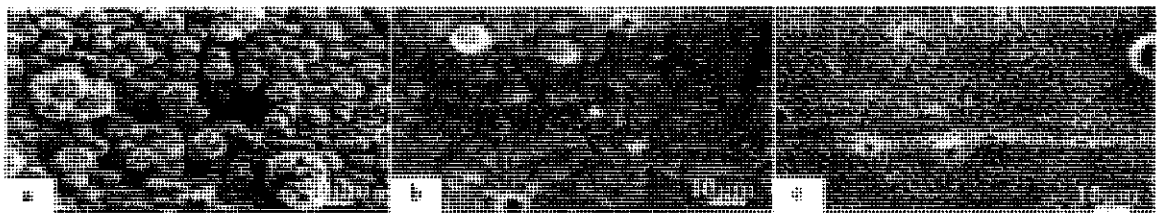

a Zn–4%Ni; *b* Zn–8%Ni; *c* Zn–16%Ni

2 *SEM micrographs of coatings*

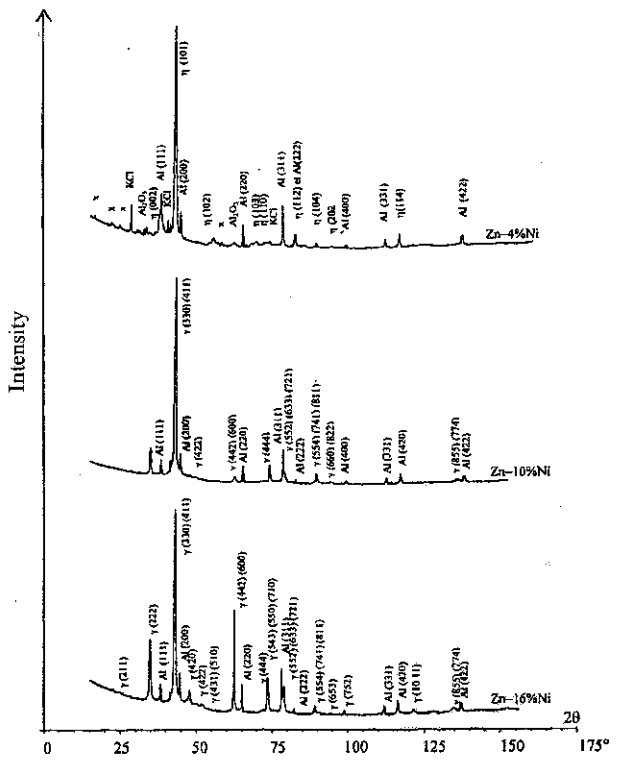

3 *Evolution of structure of deposits versus percentage of nickel*

16%Ni is monophased γ. The δ phase, expected from the thermodynamic phase diagram reported in the literature,[12] could not be identified from the X-ray data in the as deposited alloys. All the results conform with the results found in the literature.[10,13,14]

Mechanical behaviour

Measurements of the apparent hardnesses obtained are given in Fig. 4, which presents the evolution of hardness versus the ratio between indentation depth D and the thickness of the deposit e. The Zn–4%Ni coating exhibits a hardness lower than that of the substrate, which contrasts with the coatings rich in nickel. The decrease in hardness of the deposit containing more than 10%Ni when the ratio D/e increases shows the influence of the substrate. The absolute hardnesses of the coating calculated by analytical models are presented in Table 2. The models of Buckle and Jönsson–Hogmark did not give satisfactory predictions for the Zn–4%Ni coatings regardless of the value of the D/e ratio. The Buckle model seems

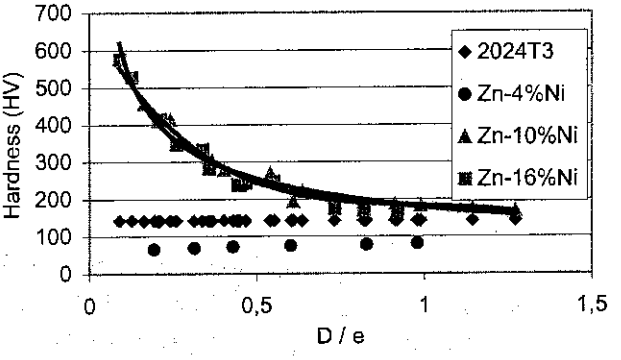

4 *Evolution of hardness versus ratio between indentation depth D and thickness of deposit e*

to work for a ratio $D/e > 0{\cdot}5$, as in the case of Zn–Ni coatings rich in nickel. The Jönsson–Hogmark model provides the best results for Zn–Ni coatings containing more than 10%Ni. These results were expected because their publications for hard coatings on a soft substrate validate these models. It has been seen previously that Zn–Ni deposits rich in nickel are harder than the EN AW2024 T3 aluminium alloy. Moreover, the model of Jönsson–Hogmark gives better predictions when the constant C takes the value $2 \sin^2 11$ (model 2 of Jönsson–Hogmark) rather than $\sin^2 22$ (model 1 of Jönsson–Hogmark). Model 2 is suggested as suitable for the case of a hard and brittle film on a soft substrate. It is assumed that the film accommodates the indenter by crack formation in the interior of the indentation. Indeed, observation of the indentations (Fig. 5) shows very well developed cracks in the close vicinity of the rim. The Chicot–Lesage model greatly underestimates the hardness of the hard deposits, which have a percentage of nickel $\geqslant 10\%$. This model seems to give more coherent values with regard to the deposit that contains 4%Ni for $D/e > 2$. To explain these results, it is necessary to refer to the starting assumptions of this model. Indeed, the Chicot–Lesage model supposes the continuity of the deformation between the coating and the substrate, and no crack is observed around the rim on the Zn–4%Ni.

Nanoindentation tests were used to determine the absolute hardness of the coatings. Indents in the cross-section of each coating with a peak displacement $\leqslant 1000$ nm were made (Fig. 6). The difference in the hardness of the coatings was obvious from the large differences in the loads reached at the maximum depth. The respective nanohardnesses of the Zn–16%Ni, Zn–8%Ni and Zn–4%Ni were 6·89 GPa, 4·2 GPa and 1·2 GPa (Fig. 7). The elastic recovery during the unloading varies with the percentage of Ni in the coating. When the percentage of Ni is higher, the release on unloading is more important. The nanohardness of the EN AW2024 T3 aluminium alloy (1·94 GPa) is higher than that of the Zn–4%Ni coating but lower than the hardness of the coatings which contain more than 8%Ni. These results confirm the previous results obtained by microindentation, namely the hardness values calculated by analytical models. Young's modulus determined by the nanoindentation test is estimated at 130 GPa for the 10 and 16%Ni coatings and 70 GPa for the Zn–4%Ni coating. All these Young's moduli were calculated with Poisson's ratio considered equal to 0·25.

The behaviour of the coatings under a scratch test at constant load was tested. Two types of mechanical behaviour were confirmed, depending

Table 2 Absolute hardness of coating calculated by analytical model

	Zn–4%Ni	Zn–10%Ni	Zn–16%Ni
Experimental data			
Microindentation	70 HV	550 HV	600 HV
Nanoindentation	114 HV	400 HV	610 HV
Analytical models			
Buckle	<0 HV	560 HV	580 HV
Jönsson–Hogmark	<0 HV	550 HV	600 HV
	<0 HV	425 HV	425 HV
Chicot–Lesage	125 HV	225 HV	225 HV

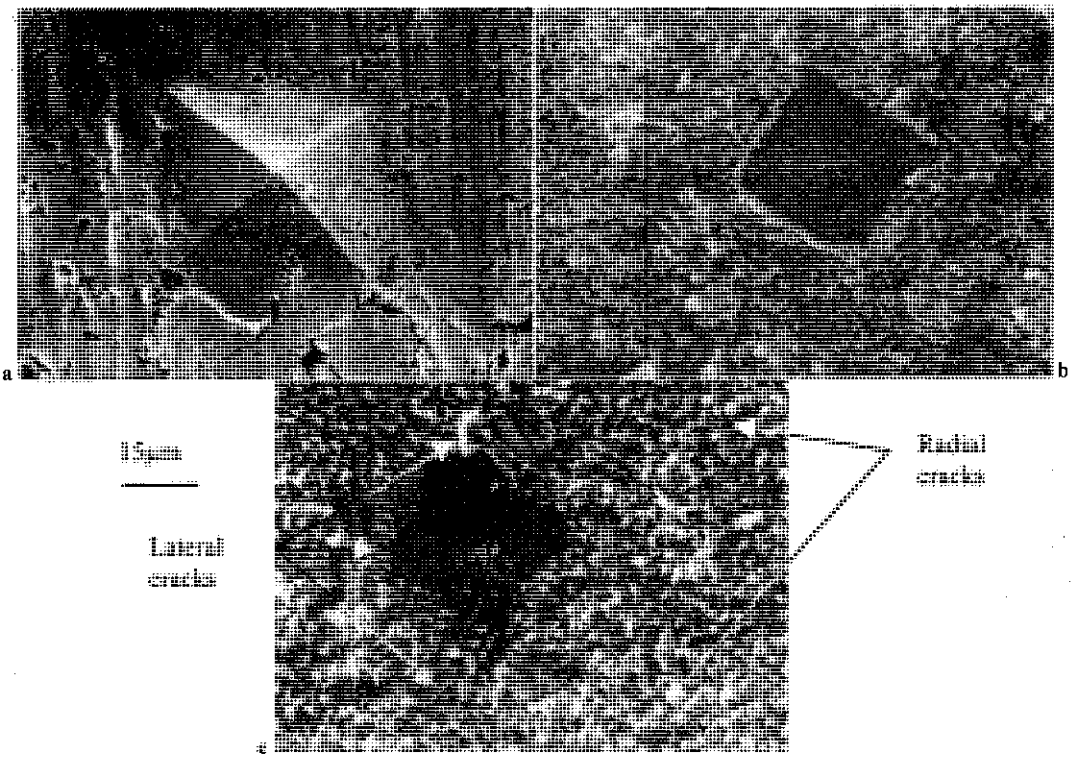

a Zn–4%Ni; *b* Zn–10%Ni; *c* Zn–16%Ni

5 *SEM micrographs of indents on coatings*

on the percentage of Ni in the coatings. The Zn–4%Ni coating buckles below the indenter without any substrate deformation. In comparison, for the Zn–16%Ni and Zn–8%Ni coatings, deformation of both the substrate and the coating were observed. These coatings exhibit a tendency to crack first in the wrinkle, then at the edge, and they finally begin to flake off. The spacing between these transverse microcracks decreases when the applied load is increased (Fig. 8). On the contrary, the Zn–4%Ni coating is plastically strained below the indenter without microcracking. The coating is pushed out to the indenter sides (Fig. 8). This different mechanical behaviour can be explained by the variation in the coating/substrate hardness H_c/H_s ratio as a function of the percentage of nickel. Obviously, this ratio is >3 for a Zn–16%Ni coating and is ~ 1 for a Zn–4%Ni coating. All these changes in the mechanical properties have an effect on the critical load L_c. For a 4%Ni coating 10 μm thick, the substrate appears at the base of the wrinkles for a critical load $\geqslant 200$ g. L_c is equal to 70 g for a Zn–16%Ni coating of the same thickness. Ahn *et al.*[15] obtained the same results for other surface treatments. They classified the mechanisms of coating removal according to whether the coating was brittle or ductile. If the coating is brittle, it is stripped

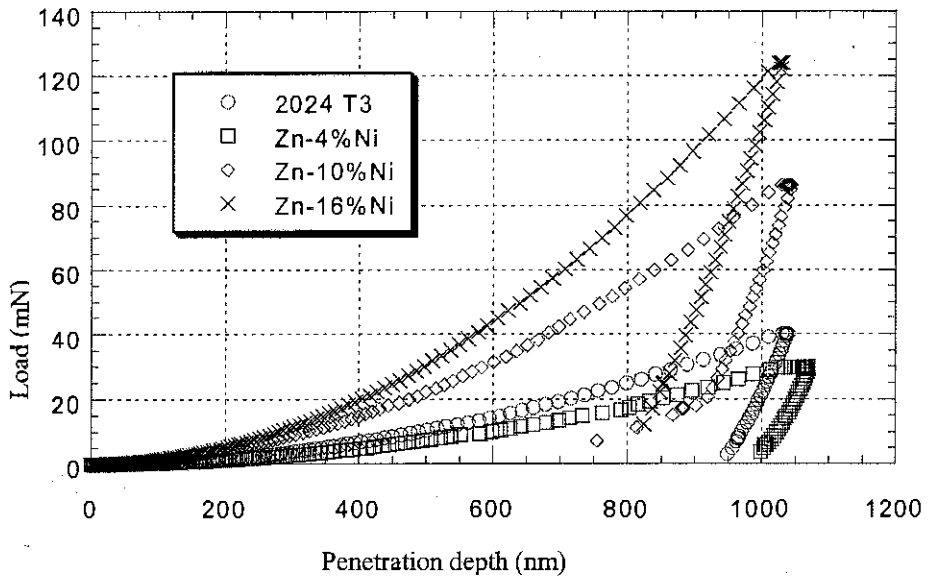

6 *Load versus indenter displacement for each coating and EN AW 2024T3 substrate*

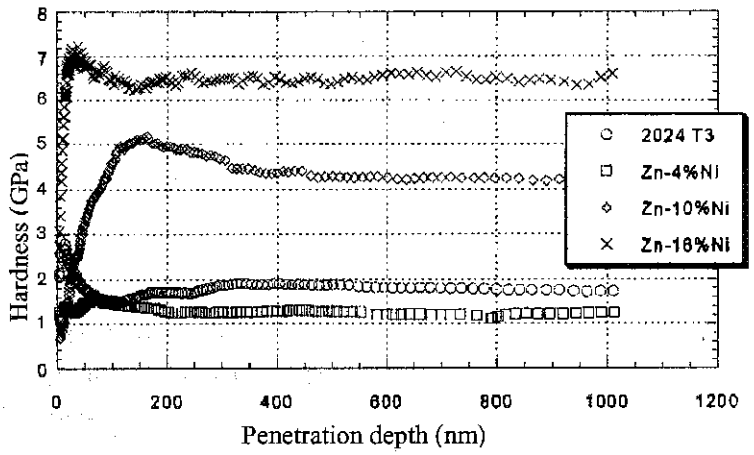

7 *Hardness for each coating and EN AW 2024T3 substrate*

completely but, if it is ductile, it is subjected to gradual thinning. The tensile residual stresses could also explain the brittle behaviour of the coating rich in nickel. The flexion test shows the favourable effect of pretreatments on the adherence of Zn–Ni onto 2024 T3 aluminium alloy (Fig. 9). The critical load is at least twice as much after these pretreatments. Decohesion takes place between the stiffener and the coating for Zn–16%Ni electrodeposited on zincate pretreated 2024 aluminium alloy. The presence of oxygen next to the interface is responsible for the loss of adherence of the deposits. Indeed, like Bories,[1] the present authors have observed by SIMS analyses (Fig. 10) oxygen at the interface hetween aluminium alloys and Zn–Ni coating for the samples without zincate pretreatment. This presence of oxygen is not obvious in the case of coatings electrodeposited after zincate pretreatment (Fig. 11). Moreover, the favourable influence of the phosphoric anodisation on the adherence of Zn–Ni deposited on EN AW2024 T3 aluminium alloy can be explained by the mechanism of mechanical interlocking between the electrodeposit and the porous oxide. Indeed, the flexion failure is localised in the anodic film, as shown by SEM. A certain amount of Zn–Ni coating remains in the porosity. The SIMS analysis of the interface shows that penetration of the coating through the anodic film existed (Fig. 12). However, thermodynamic adhesion supported by surface energy measurements must not be neglected. Indeed, comparison of the various results obtained according to the surface preparation (Table 3) highlights a variation in the dispersive and non-dispersive terms of the surface energy. The dispersive component γ_S^D is usually low in the case of a rough surface. It increases after a total scouring of the substrate or anodisation but is weak after zincate treatment. The contribution of the non-dispersive interactions I_{Swater}^{ND} to the total work of adhesion increases in a progressive way compared with that of a rough surface, whatever the processing carried out. Taking into account the high values of I_{Swater}^{ND} usmg the method with one liquid, one could question the validity of the results. Indeed, it

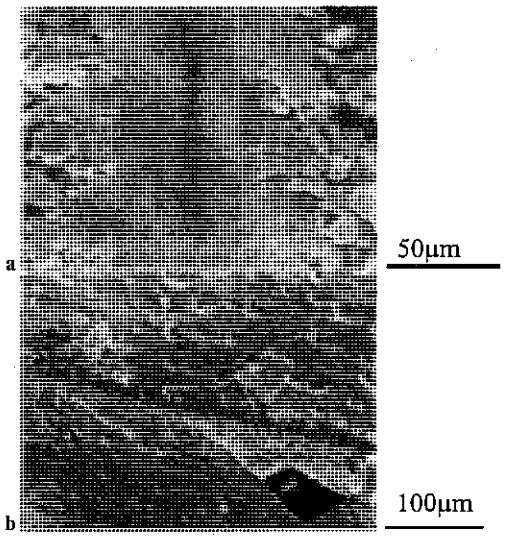

a Zn–4%Ni coating 300 g; *b* Zn–16%Ni coating 45 g

8 *SEM micrographs of wrinkles after scratch test*

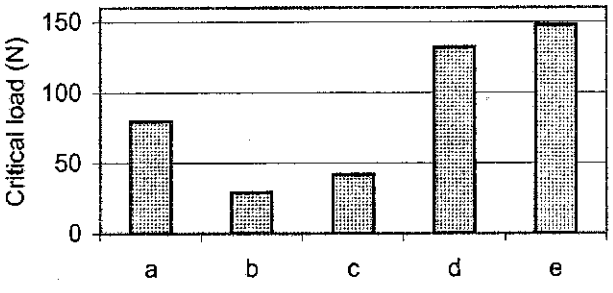

a 4%Ni; *b* 8%Ni; *c* 16%Ni; *d* 16%Ni on EN AW2024 zincate pretreated; *e* 16%Ni on EN AW2024 anodised

9 *Critical load for coatings electrodeposited directly onto 2024 aluminium alloy*

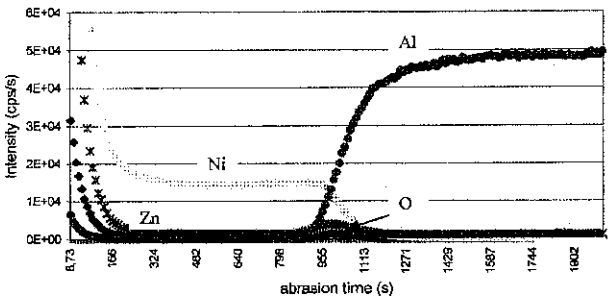

10 *SIMS analysis of Zn–16%Ni electrodeposited onto 2024 aluminium alloy*

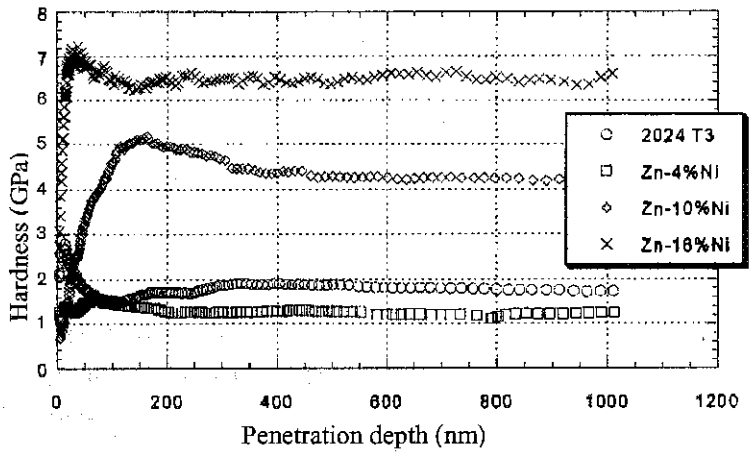

7 *Hardness for each coating and EN AW 2024T3 substrate*

completely but, if it is ductile, it is subjected to gradual thinning. The tensile residual stresses could also explain the brittle behaviour of the coating rich in nickel. The flexion test shows the favourable effect of pretreatments on the adherence of Zn–Ni onto 2024 T3 aluminium alloy (Fig. 9). The critical load is at least twice as much after these pretreatments. Decohesion takes place between the stiffener and the coating for Zn–16%Ni electrodeposited on zincate pretreated 2024 aluminium alloy. The presence of oxygen next to the interface is responsible for the loss of adherence of the deposits. Indeed, like Bories,[1] the present authors have observed by SIMS analyses (Fig. 10) oxygen at the interface hetween aluminium alloys and Zn–Ni coating for the samples without zincate pretreatment. This presence of oxygen is not obvious in the case of coatings electrodeposited after zincate pretreatment (Fig. 11). Moreover, the favourable influence of the phosphoric anodisation on the adherence of Zn–Ni deposited on EN AW2024 T3 aluminium alloy can be explained by the mechanism of mechanical interlocking between the electrodeposit and the porous oxide. Indeed, the flexion failure is localised in the anodic film, as shown by SEM. A certain amount of Zn–Ni coating remains in the porosity. The SIMS analysis of the interface shows that penetration of the coating through the anodic film existed (Fig. 12). However, thermodynamic adhesion supported by surface energy measurements must not be neglected. Indeed, comparison of the various results obtained according to the surface preparation (Table 3) highlights a variation in the dispersive and non-dispersive terms of the surface energy. The dispersive component γ_S^D is usually low in the case of a rough surface. It increases after a total scouring of the substrate or anodisation but is weak after zincate treatment. The contribution of the non-dispersive interactions I_{Swater}^{ND} to the total work of adhesion increases in a progressive way compared with that of a rough surface, whatever the processing carried out. Taking into account the high values of I_{Swater}^{ND} usmg the method with one liquid, one could question the validity of the results. Indeed, it

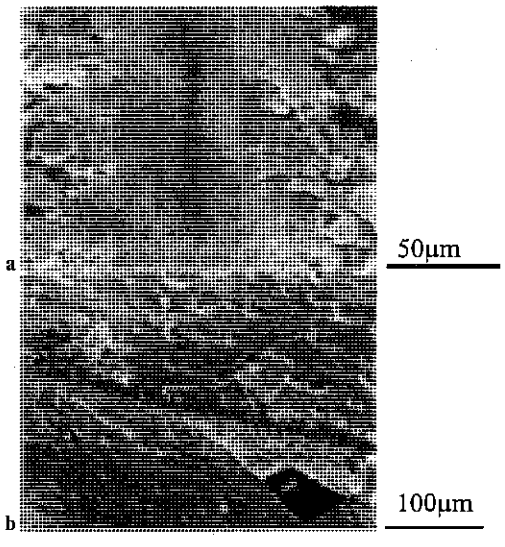

a Zn–4%Ni coating 300 g; *b* Zn–16%Ni coating 45 g

8 *SEM micrographs of wrinkles after scratch test*

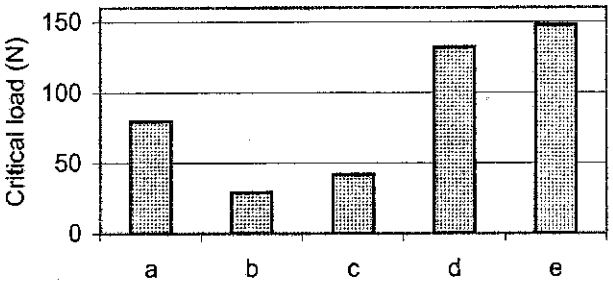

a 4%Ni; *b* 8%Ni; *c* 16%Ni; *d* 16%Ni on EN AW2024 zincate pretreated; *e* 16%Ni on EN AW2024 anodised

9 *Critical load for coatings electrodeposited directly onto 2024 aluminium alloy*

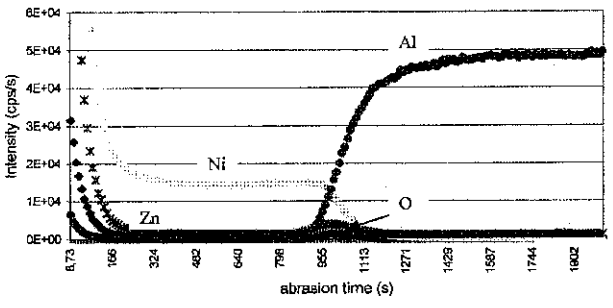

10 *SIMS analysis of Zn–16%Ni electrodeposited onto 2024 aluminium alloy*

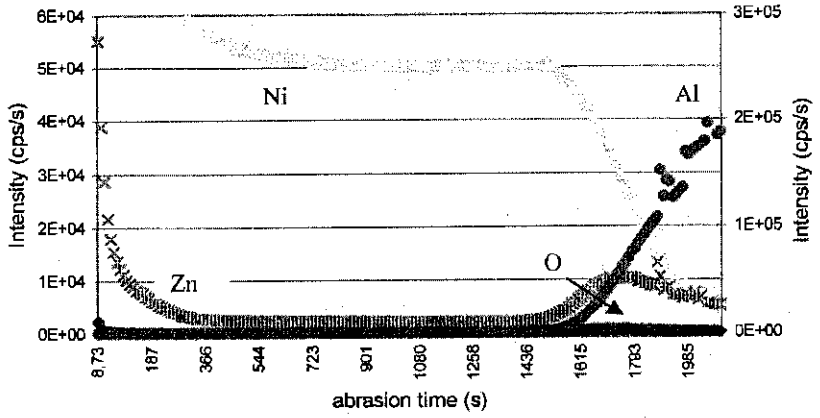

11 *SIMS analysis of Zn–16%Ni electrodeposited onto zincated 2024 aluminium alloy*

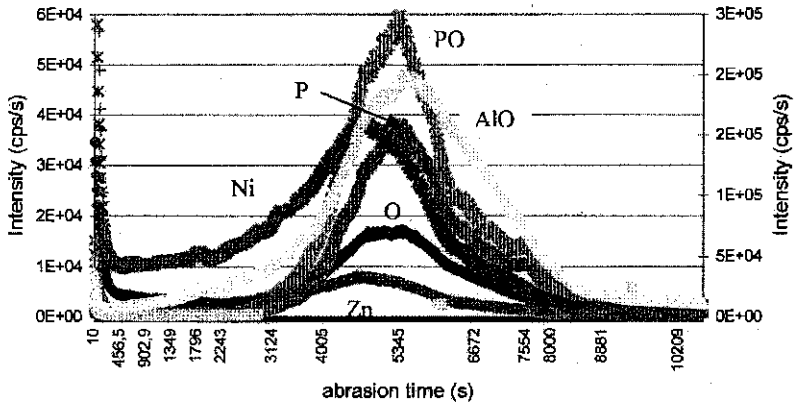

12 *SIMS analysis of Zn–16%Ni electrodeposited onto anodised 2024 aluminium alloy*

is important to specify that the pressure of the spreading out effect was neglected. To avoid this problem, surface energy measurements were carried out according to the method with two liquids. Water distilled (pH = 5·7) droplets were deposited on the surfaces studied, which were placed in an enclosure filled with octane. Since octane has a surface energy ($\gamma_{octane} = 21{\cdot}3$ mJ m^{-2}) close to the dispersive term of surface energy in presence of water ($\gamma^{D}_{water} = 21$ mJ m^{-2}), the term of the equation $\sqrt{\gamma^{D}_{water}} - \sqrt{\gamma_{octane}}$ used in this method is almost equal to zero. Consequently, the acid–base term of the surface energy W^{AB}_{Swater} can be estimated by

$$\gamma_{water} - \gamma_{octane} + \gamma_{water/octane} \cos\theta_{water/octane} \approx W^{AB}_{Swater}$$

The calculated values of W^{AB}_{Swater} appear in Table 4. These values are more representative of the non-dispersive effects than of those presented previously. If these values are compared with those obtained from the method with one liquid, the strong influence of the pressure of spreading out in the case of zincated and pickled surfaces appeared. The value of W^{AB}_{Swater} for the anodised surface is the most important, favouring Zn–Ni adherence.

CONCLUSION

Several Zn–Ni coatings electrodeposited on 2024 T3 aluminium alloy were characterised according to the percentage of Ni and their pretreatment. The surface smoothing of the coating was due to a microstructural refinement when the percentage of Ni increased. A Zn–16%Ni coating exhibited brittle behaviour, while Zn–4%Ni showed ductile behaviour under a scratch test. This was explained by the hardness difference and more precisely by the ratio between Young's modulus and the hardness. The mechanical properties of the deposits must be accommodated to obtain correct adherence. The favourable influence of pretreatments such as zincate or phosphoric anodisation on the adherence was emphasised. Zincate pretreatment is known to avoid the natural aluminium oxide formed on the surface of the substrate. To explain the good adherence owing to phosphoric anodisation,

Table 3 Values of γ^{D}_{S} and I^{ND}_{Swater} obtained by Fowkes method according to various pretreatments carried out on alloy EN AW2024 T3

	γ^{D}_{S}, mJ m^{-2}	I^{ND}_{Swater}, mJ m^{-2}
Raw surface of alloy	32·3±1·34	47·4±3·35
Scouring surface of alloy	40·25±1·97	72±1·77
Anodised surface of alloy	39·7±2·76	82±1·29
Zincated surface of alloy	32·8±2·46	82·7±2·03

Table 4 Values of W^{AB}_{Swater} obtained by method with two liquids according to various pretreatments carried out on alloy EN AW2024 T3

	W^{AB}_{Swater}, mJ m^{-2}
Raw surface of alloy	32·5±0·55
Scouring surface of alloy	35·85±0·7
Anodised surface of alloy	87·8±0·67
Zincated surface of alloy	10·4±0·16

mechanical interlocking and high surface energy were discussed.

APPENDIX

Buckle model

$$H_c = H_s + \left(\frac{\sum_{i=1}^{k} P_i}{\frac{12}{\sum_{i=1} P_i}} \right) (H_f - H_s)$$

where H_f is the deposit hardness and P_i is the experimental coefficient for each layer under the indent.

Jönsson–Hogmark model

$$H_c = H_s + \left[2C \frac{e}{d} - \left(C \frac{e}{d} \right)^2 \right] (H_f - H_s)$$

where C is a constant which depends on the deposit deformation

$C = \sin^2 22$ for hard substrate and plastically deforming film

$C = 2\sin^2 11$ for hard and brittle deposit on soft substrate

Chicot–Lesage model

$$H_c = H_s + \frac{1}{2} \left\{ 3 \operatorname{tg}^{1/3} \zeta \frac{e}{d} \left[\left(\frac{H_f}{E_f} \right)^{1/2} + \left(\frac{H_s}{E_s} \right)^{1/2} \right] \right\} \times (H_f - H_s)$$

where ζ is the ½ angle of the indenter tip, E_s is Young's modulus of the substrate, and E_f is Young's modulus of the deposit.

ACKNOWLEDGEMENTS

The authors gratefully acknowledge Mr S. Faure (Centre d'Etude des Surfaces et d'Analyse des Matériaux de l'Université de Marne La Vallée) for the SIMS analyses and the AMSA laboratory for financial support.

REFERENCES

1. C. BORIES: PhD thesis, Université Paul Sabatier, No. 3233, Toulouse, 1998.
2. F. M. FOWKES: *Rubber Chem. Technol.*, 1984, **57**, 328.
3. J. SCHULTZ, K. TSUTSUMI and J. B. DONNET: *J. Colloid Interface Sci.*, 1977, **59**, 272.
4. H. BUCKLE: 'Publications Scientifiques et Techniques du Ministère de l'Air N.T. ', 90, Paris, 1960.
5. B. JONSSON and S. HOGMARK: *Thin Solid Films*, 1984, **114**, 257.
6. J. LESAGE, D. CHICOT, Y. BENARIOUA, P. ARAUJO and P. DEMARECAUX: *Rev. Métall. CIT Sci. Génie Mater.*, 1999, 1121.
7. G. M. PHARR and W. C. OLIVER: *Mater. Res. Soc. Bull.*, 1992, **17**, 28.
8. P. A. STEINMANN and H. E. HINTERMANN: *J. Vac. Sci. Technol. A.*, 1985, **A3**, 2394.
9. A. A. ROCHE, J. R. BEHME and J. S. SOLOMON: *Int. J. Adhes. Adhes.*, 1982, **2**, 249.
10. S. BRUETHOTTELAZ: PhD thesis, Université Paul Sabatier, Toulouse, 1996.
11. J. K. CRITCHLEY and S. DENTON: *J. Inst. Metals*, 1971, **99**, 26.
12. G. O. MALLORY: *Plat. Surf. Finish.*, 1985, **72**, 86.
13. A. M. ALFANTAZI, G. BREHAUT and U. ERB: *Surf. Coat. Technol.*, 1997, **89**, 239.
14. M. KURACHI, K. FUJIWARA and T. TANAKA: *Interfinish Surf.*, 1973, **72**, 152.
15. J. AHN, K. L. MITTAL and R. H. MACQUEEN: 'Adhesion measurements in thin films', 134; 1978, ASTM.